HEAT TRANSFER SIMULATION AND PERFORMANCE OPTIMIZATION OF PLATE-TYPE PHASE CHANGE ENERGY STORAGE UNIT

by

Long MIAO[a], Rui WAN[b,c*], Zhen LIU[b,c], and Huawei WU[b,c]

[a] School of Mechanical and Electrical Engineering,
Xuzhou University of Technology, Jiangsu, China
[b] Hubei Key Laboratory of Power System Design and Test for Electrical Vehicle,
Hubei University of Arts and Science, Xiangyang, China
[c] School of Automotive and Traffic Engineering,
Hubei University of Arts and Science, Xiangyang, China

Original scientific paper
https://doi.org/10.2298/TSCI230828107M

As the core of the phase change energy storage technology, the heat transfer performance of the phase change energy storage unit has an important impact on the operating efficiency of the energy storage system. In this study, a 3-D CFD model of the plate-type phase change energy storage unit is established to simulate the melting process of paraffin wax. Three types of plate-type phase change energy storage unit models are established, without ribs, single rib, and double ribs. The influence of cylindrical rib on natural convection melting process of paraffin is studied, which provides the basis for the design and performance optimization of plate-type phase change energy storage unit, and improve its application value. The results show that the melting time of paraffin in the energy storage unit without ribs is 858 seconds , and the melting time is shortened to 827~842 seconds after adding single rib. The melting time of paraffin wax with single rib is lower than that with double ribs. For the plate-type phase change energy storage unit, adding ribs at the central section can effectively improve the melting rate of phase change material. The single rib A located at the lower part of the central section has the greatest promotion effect on paraffin melting. The key to enhance the phase change heat transfer process in plate-type phase change energy storage unit is the paraffin in the lower half of the symmetry plane.

Key words: *plate-type phase change energy storage unit, ribs, paraffin wax, natural convection, numerical simulation*

Introduction

In the process of development and utilization of various energy sources, there are often certain temporal and spatial differences between energy supply and demand, such as the peak-valley difference of grid load. For RES such as wind, solar and tidal energy, there is greater volatility in energy supply and greater imbalance between energy supply and demand. Solid-liquid phase change energy storage technology has the advantages of high heat storage density, good equipment compactness and easy management, which can effectively improve

* Corresponding author, e-mail: wanrui7035@163.com

the volatility of energy supply and enhance the stability of energy supply [1, 2]. Phase change energy storage technology has been widely used in buildings [3], solar heating systems [4, 5], waste heat recovery systems [6, 7], and air conditioning systems [8, 9].

As the core of phase change energy storage technology, the heat transfer performance of phase change energy storage unit (PCESU) has an important impact on the operating efficiency of energy storage system. Plate-type phase change energy storage units (P-PCESU) and shell and tube PCESU are the most commonly used forms of PCESU [10, 11]. The enhancement of heat transfer performance of the P-PCESU has attracted the attention of some researchers. Zhou *et al.* [12] designed a cascade phase change heat storage model and numerically simulated its internal heat transfer process. The results showed that the position of the phase change material had a significant impact on the heat transfer characteristics, and the convective heat transfer between the lower and middle phase change materials played a key role in the overall melting rate of the heat storage unit.

The current research hotspot for enhancing heat transfer in energy storage units is to add materials with strong thermal conductivity to substrates such as paraffin to prepare composite phase change materials. Yang *et al*. [13] prepared a metal foam-paraffin composite phase change material, and experimentally studied its phase change heat transfer process. The results show that the uniformity of the internal temperature distribution of the composites is improved, the heat flux is significantly increased, and the poor heat transfer performance of the bottom during the melting process of pure paraffin wax is improved. Wang *et al*. [14] studied the melting solidification cycle process of composite phase change materials using visual experimental methods. The results show that the composite phase change material can help to improve the latent heat storage capacity and increase the total heat storage of the heat storage unit. Shafee *et al*. [15] studied the heat release process during water solidification, and added CuO particles to the water to prepare nanoparticle-reinforced phase change materials. With the increase of nanomaterial concentration, the solidification time tends to decrease. The results show that the addition of CuO nanopowder reduces the solidification time by 14.39%.

Structural optimization of phase change heat transfer units is also an important research direction. Kamkari *et al*. [16] studied the melting process of phase change materials in rectangular containers with different inclination angles, and the results showed that the inclination of the shell has a significant effect on the formation of natural convection, and therefore also has a great influence on the heat transfer rate and melting time of phase change materials. Gurel [17] studied the P-PCESU made of corrugated steel plate and compared it with the performance of the cylindrical energy storage unit, and found that the phase change material in the P-PCESU has a short solidification time, reducing the solidification time by up to 63%. Lin *et al*. [18] proposed a new P-PCESU, in which a distributed water flow channel is provided in the substrate for charging or discharging the phase change material. The experimental results show that the pillow plate type heat exchanger has good compactness and heat transfer performance.

In the published research, on the one hand, the composite phase change material is prepared by adding enhanced heat transfer materials to the paraffin substrate, and on the other hand, the P-PCESU itself is studied to optimize its structure and enhance the heat transfer performance inside the energy storage unit. In this study, a 3-D CFD model of the P-PCESU is established, and the melting process of paraffin in the P-PCESU is simulated and analyzed. Then, cylindrical ribs are added to P-PCESU, and the influence of cylindrical ribs on the natural convective melting process of paraffin is studied, and the number and distribution of ribs are optimized, so as to improve the heat transfer performance of P-PCESU, which provides a basis for the performance optimization of P-PCESU.

Simulation model

Physical model

The PCESU in this study is a flat plate type, with aluminum as the outer shell material and paraffin as the internal filling material. The structure of the energy storage unit is shown in fig. 1.

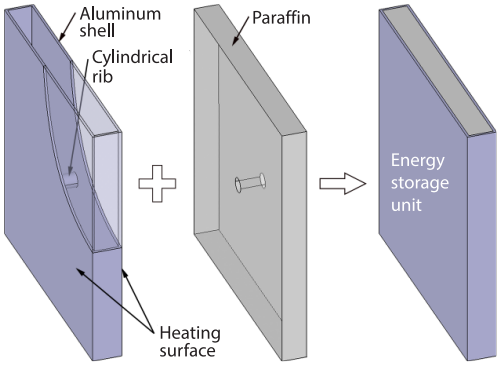

Figure 1. Plate-type phase change energy storage unit

The volume of paraffin is 100 mm × 100 mm × 10 mm, and the thickness of the aluminum shell is 1 mm. The energy storage unit has heating surfaces on both sides, which heat the internal paraffin to melt it. In order to enhance the heat transfer performance of the energy storage unit, cylindrical ribs are added in the cavity to compare and study the strengthening effect of different numbers and arrangement of ribs on the heat transfer performance of the energy storage unit.

The cylindrical ribs in the energy storage unit are divided into two groups, single ribs and double ribs, and each group has three different rib arrangements. The diameter of the single rib is 6 mm, the diameter of each rib in the double rib group is 4.25 mm, and the total volume of the ribs is the same. The single rib is located in the center section of the energy storage unit, while the double ribs are symmetrically distributed on both sides of the center section. In the simulation process, four temperature monitoring points are set in the energy storage unit, and the measurement points are located on the symmetrical surface of the energy storage unit. The location of the ribs and temperature measurement points is shown in fig. 2 in mm.

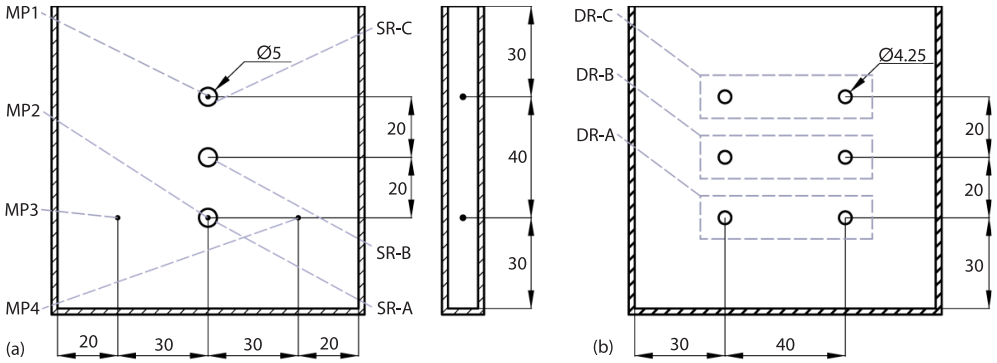

Figure 2. Location of ribs and temperature measurement points (MP); (a) single rib (SR) and (b) double ribs (DR)

Mathematical model

The melting process of paraffin belongs to the problem of phase change heat transfer, and the solid-liquid interface during the melting process is a region where two phases coexist. The density of solid paraffin wax decreases after melting, and natural convection occurs in high temperature liquid paraffin wax under the effect of buoyancy. The enthalpy porosity method [19, 20] is applied to simulate the melting process of paraffin, and the liquid fraction parameter is used to describe the changes in the solid-liquid interface. The control equations are:

$$\frac{\partial \rho}{\partial t}+\frac{\partial(\rho u)}{\partial x}+\frac{\partial(\rho v)}{\partial y}+\frac{\partial(\rho w)}{\partial z}=0 \tag{1}$$

$$\begin{aligned}
\rho\left(\frac{\partial u}{\partial t}+u\frac{\partial u}{\partial x}+v\frac{\partial u}{\partial y}+w\frac{\partial u}{\partial z}\right)&=\mu\left(\frac{\partial^2 u}{\partial x^2}+\frac{\partial^2 u}{\partial y^2}+\frac{\partial^2 u}{\partial z^2}\right)-\frac{\partial p}{\partial x}+S_u\\
\rho\left(\frac{\partial v}{\partial t}+u\frac{\partial v}{\partial x}+v\frac{\partial v}{\partial y}+w\frac{\partial v}{\partial z}\right)&=\mu\left(\frac{\partial^2 v}{\partial x^2}+\frac{\partial^2 v}{\partial y^2}+\frac{\partial^2 v}{\partial z^2}\right)-\frac{\partial p}{\partial y}+S_v\\
\rho\left(\frac{\partial w}{\partial t}+u\frac{\partial w}{\partial x}+v\frac{\partial w}{\partial y}+w\frac{\partial w}{\partial z}\right)&=\mu\left(\frac{\partial^2 w}{\partial x^2}+\frac{\partial^2 w}{\partial y^2}+\frac{\partial^2 w}{\partial z^2}\right)-\frac{\partial p}{\partial z}+S_w
\end{aligned} \tag{2}$$

$$\rho\left(\frac{\partial H}{\partial t}+u\frac{\partial H}{\partial x}+v\frac{\partial H}{\partial y}+w\frac{\partial H}{\partial z}\right)=\frac{\lambda}{c_p}\left(\frac{\partial^2 H}{\partial x^2}+\frac{\partial^2 H}{\partial y^2}+\frac{\partial^2 H}{\partial z^2}\right)+S_h \tag{3}$$

where u, v, and w are the components of velocity in the x-, y-, and z-directions, respectively, ρ [kgm^{-3}] – the density of paraffin wax, μ [Pa·s] – the dynamic viscosity of paraffin wax, λ [Wm^{-1}K^{-1}] – the thermal conductivity of paraffin wax, c_p [kJkg^{-1}K^{-1}] – the specific heat capacity of paraffin, p [Pa] – the pressure, S_u, S_v, and S_w are the source terms of the momentum equation in the x-, y-, and z-directions, respectively, and S_h is the source term of the energy equation.

The enthalpy equation:

$$\begin{aligned}
H&=h+\Delta H\\
h&=h_{ref}+\int_{T_{\mathrm{ref}}}^{T} c_p \mathrm{d}T\\
\Delta H&=\beta L
\end{aligned} \tag{4}$$

where H [kJkg^{-1}] is the specific enthalpy, h [kJkg^{-1}] – the sensible enthalpy, ΔH [kJkg^{-1}] – the latent enthalpy, L [kJkg^{-1}] – the latent heat of phase transition of paraffin, T_{ref} [K] – the reference temperature, h_{ref} [kJkg^{-1}] – the enthalpy at the reference temperature, and β – the volume fraction of liquid paraffin.

Simulation method

The P-PCESU shown in fig. 1 is meshed. Poly-Hexcore grid is generated using FLUENT meshing. In order to verify the independence of the grid, the calculation domain is divided into 40000-500000 grids, and simulation calculations are conducted for 500 seconds under the same boundary conditions. The temperature variations at measurement Points 1 and 2 are shown in tab. 1. After the number of grids exceeds 250000, the calculation results tend to stabilize. Taking into account the accuracy and time of the calculation, a grid division scheme with a grid number of 250000 was selected.

Table 1. Grid independence verification

Grid number [·10^3]	40	80	160	250	500
Temperature of MP1 [K]	324.859	325.244	325.452	325.597	325.648
Temperature of MP2 [K]	324.768	325.018	325.256	325.465	325.527

During the calculation process, the heating surfaces on both sides of the energy storage unit are set as constant temperature surfaces, with a heating temperature of 343 K. The other

surfaces are insulated walls. The initial temperature of the energy storage unit is 293 K. During the calculation process, the influence of gravity is considered, and the direction of gravity is in the negative *z*-direction.

In the process of numerical simulation, a 3-D discrete, implicit unsteady state solver is used to solve the problem. The time step for simulation calculation is 1 second. The convergence criteria are continuity, residual of momentum equation, and energy equation, with thresholds of 10^{-3}, 10^{-3}, and 10^{-6}, respectively. The energy equation and solidification/melting model were loaded during the simulation process. The SIMPLE algorithm is used for the coupling of pressure and velocity. The numerical simulation was conducted using commercial software ANSYS FLUENT, version R2021.

The phase change material is paraffin, and its physical properties are shown in tab. 2. The housing material of the energy storage unit is aluminum, the thermal conductivity is 202.4 W/mK, the density is 2719 kg/m^3, and the specific heat capacity is 871 J/kgK. In order to consider natural convection, Boussinesq hypothesis is adopted for paraffin density. In the solid-liquid mixing zone, the thermal conductivity and specific heat capacity of paraffin are treated as functions of temperature:

$$c_p = \begin{cases} 2464 & T < T_s \\ 162T - 50186 & T_s < T < T_\ell \\ 2950 & T > T_\ell \end{cases} \tag{5}$$

$$\lambda = \begin{cases} 0.28 & T < T_s \\ -0.0467T + 15.457 & T_s < T < T_\ell \\ 0.14 & T > T_\ell \end{cases} \tag{6}$$

where T_ℓ [K] is the liquidus temperature of the material and T_s [K] – the solidus temperature of the material.

Table 2. Physical properties of paraffin

Physical properties	Unit	Value
Solid specific heat capacity, $c_{p,s}$	[Jkg^{-1}K^{-1}]	2464
Liquid specific heat capacity, $c_{p,\ell}$	[Jkg^{-1}K^{-1}]	2950
Solid state density, ρ_s	[kgm^{-3}]	900
Liquid density, ρ_ℓ	[kgm^{-3}]	773
Thermal expansion coefficient, α	[K^{-1}]	0.001
Dynamic viscosity, μ	[Pa·s]	0.03
Solid state thermal conductivity, λ_s	[Wm^{-1}K^{-1}]	0.28
Liquid thermal conductivity, λ_ℓ	[Wm^{-1}K^{-1}]	0.14
Solidus temperature, T_s	[K]	325
Liquidus temperature, T_ℓ	[K]	328
Latent heat, L	[kJkg^{-1}]	205.6

In order to verify the accuracy of the simulation method, the P-PCESU A3 and A5 from [9] are modeled and simulated, and the simulation boundary conditions were the same as in the experiment. The comparison of the temperature variation is shown in fig. 3. The simula-

tion results of A3 and A5 are both consistent with the experimental data trends. The maximum relative error of A3 is 5.3%, and that of A5 is 6.7%. The accuracy of the simulation model calculation results is good, which can be used for subsequent simulation research.

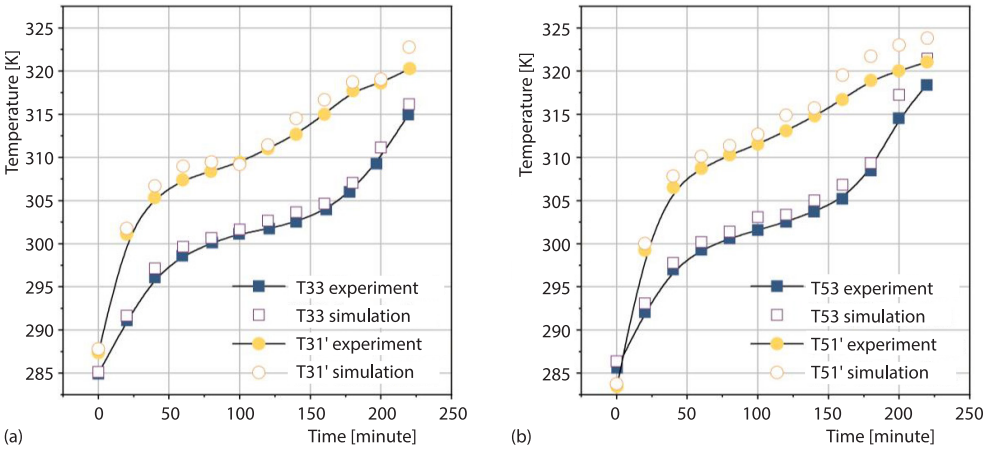

Figure 3. Comparison of simulation results and experimental data; (a) plate configuration A3 and (b) plate configuration A5

Results and discussion

Ribless

Firstly, the melting of paraffin without ribs is simulated and analyzed. Figure 4 shows the variation of the volume fraction of liquid paraffin in the symmetrical plane of the P-PCESU over time. The upper part of the paraffin in the energy storage unit melts quickly and has been completely melted after heating for 600 seconds. Because the molten paraffin flows upward under the action of natural convection, the melting rate of the paraffin in the upper part is accelerated. The paraffin in the lower half of the energy storage unit has not yet melted after heating for 800 seconds.

The average Nusselt number, during melting [21]:

$$\overline{\mathrm{Nu}} = \frac{\rho_l L W_{\mathrm{PCM}} H_{\mathrm{PCM}} \left(\frac{\mathrm{d}\beta}{\mathrm{d}\tau} \right)}{\left(t_{\mathrm{w}} - t_{\mathrm{m}} \right) \lambda_\ell} \tag{7}$$

where W_{PCM} [m] is the width of the phase change element, H_{PCM} [m] – the height of the phase change unit, t_{w} [K] – the heating wall temperature, and t_{m} [K] – the melting point of paraffin.

Figure 5 shows the average Nusselt number calculated by eq. (7) and liquid paraffin volume fraction over time. The average Nusselt number decreases sharply over time, and then slowly decreases. Because in the early stage of heating, the main heat transfer mechanism inside the energy storage unit is heat conduction, and the thermal resistance increases with the increase of volume fraction of liquid paraffin, resulting in a sharp decrease in Nusselt number. With the increase of liquid paraffin, natural convection in the energy storage unit gradually dominates, but the heat transfer enhancement caused by natural convection is weaker than the heat transfer hindrance combined by the increase of thermal resistance and the decrease of heat transfer temperature difference, so the average Nusselt number decreases slowly.

The liquid volume fraction in the energy storage unit gradually increases with the heating process, and the liquid volume fraction reaches 1 at 855 seconds, that is, the paraffin in the energy storage unit is completely melted. The variation trend of liquid volume fraction in the symmetric plane is the same, but at the same time, it is lower than the overall liquid volume fraction. Because the paraffin in the symmetrical plane is far from the heating surface, the melting rate is slow. The volume fraction of liquid paraffin in the symmetrical surface reaches 0.96 after heating for 800 seconds, and the liquid volume fraction in the entire energy storage unit is 0.98.

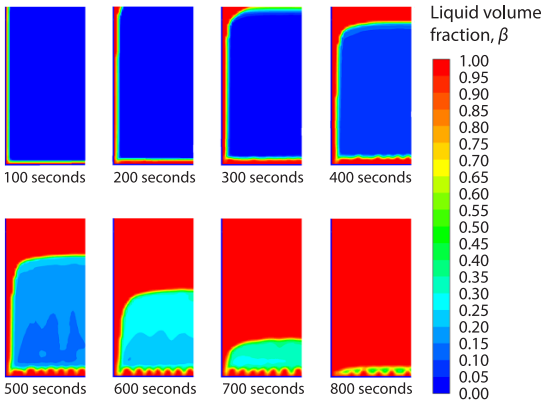

Figure 4. Contour plot of liquid volume fraction without ribs

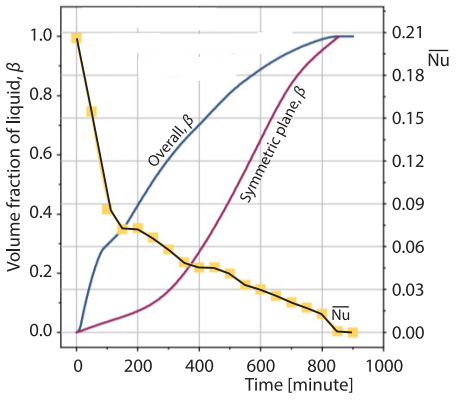

Figure 5. Average Nusselt number and liquid paraffin volume fraction

Single rib

A single cylindrical rib with a diameter of 6 mm and a rib position height of 30 mm, 50 mm and 70 mm is added to the energy storage unit. The effect of ribs in different positions on the liquid volume fraction of the melting process is shown in fig. 6.

The 400 seconds after the heating starts, the paraffin around the ribs is partially melted, and the proportion of liquid paraffin wax is higher than when there are no ribs. At 500 seconds, the paraffin around the ribs melts further, forming a liquid paraffin area in the middle of the solid paraffin. Due to natural convection, paraffin above the ribs melts faster than those below the ribs. Single rib A is located in the lower part of the energy storage unit, which heats the paraffin wax that melts slowly in this area, which effectively increases the melting rate of paraffin in the energy storage unit. At 600 seconds and 800 seconds, the unmelted paraffin of SR-A is less than that of the other two single-rib arrangements. The time required for paraffin to melt completely is 827 seconds for SR-A, 835 seconds for SR-B, and 842 seconds for SR-C. Therefore, when the position of the ribs is low, the melting speed of paraffin in

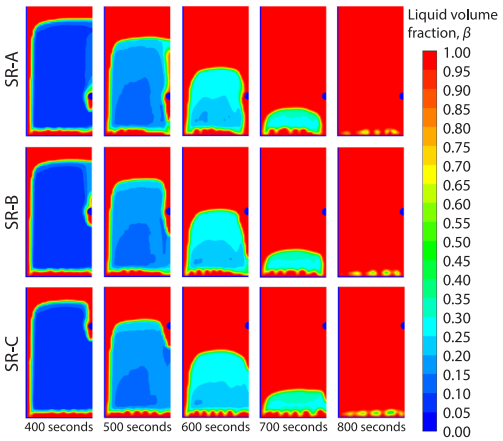

Figure 6. Variation of liquid volume fraction with single rib

the energy storage unit is greatly increased. The melting time of all three groups of SR is lower than that of no ribs, because the presence of ribs increases the heat exchange area and makes the internal heating of paraffin wax more uniform.

Figure 7 shows the temperature variation at the measuring points (MP1, MP3). The MP1 is located in the upper part of the energy storage unit, and the distance between the positions of SR-A, SR-B, and SR-C and MP1 decreases sequentially, so the MP1 of SR-A melts at the latest. The MP1 of SR-C overlaps the position of the rib, so its temperature rises rapidly after the heating starts and remains consistent with the heating surface temperature. After heating for 510 seconds, the temperature of MP1 in SR-A rises to 328 K, and the paraffin at the corresponding position completely melts. Subsequently, it rapidly heats up under the convection heat transfer of liquid paraffin; The temperature of MP1 of SR-B increased to 328 K after heating for 450 seconds, and the subsequent heating rate was lower than that of SR-A.

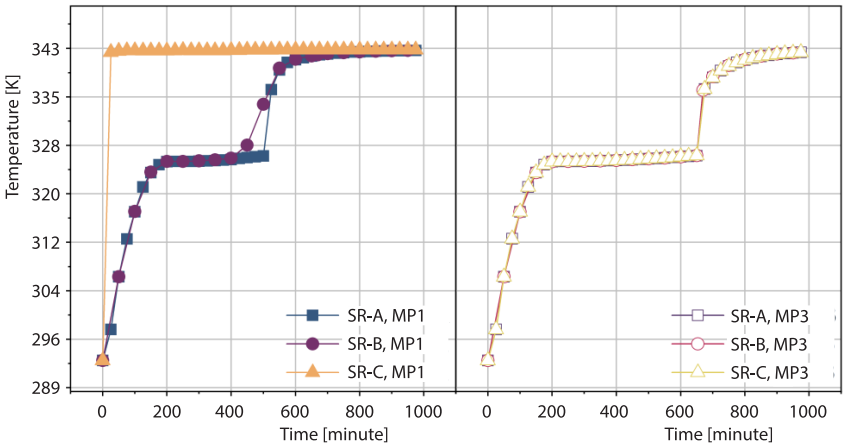

Figure 7. Temperature variation of measuring point with single rib

Double ribs

Figure 8 shows the effect of double ribs (DR) on the liquid volume fraction. Similar to the situation of the SR group, after 500 seconds of heating, the liquid volume fraction in the energy storage unit is DR-A > DR-B > DR-C, and the lower ribs had a better effect on paraffin melting. When heated for 600 seconds, the solid paraffin wax at the bottom of DR-A and DR-B has been divided by liquid paraffin, while the unmelted paraffin is still connected in DR-C, and the melting rate is significantly lower than that of the other two rib arrangement. It is worth noting that compared with the SR group, the unmelted area at 800 seconds in the DR group is larger. Because the SR is located on the central surface of the energy storage unit, it is able to heat the paraffin wax that melts the slowest. The ribs of the double rib groups are distributed symmetrically along the center of the energy storage unit, which reduces the heating effect. The total melting time of DR-A, DR-B and DR-C is 843 seconds, 849 seconds, and 858 seconds, respectively.

The melting time of paraffin wax with different rib arrangements is shown in fig. 9. The melting time of DR-C is the same as that without ribs, and the other five rib arrangements all reduce the time for complete melting of paraffin. The melting time of the SR group is lower than that of the DR group, indicating that for the P-PCESU, the key to improving the melting speed is to promote the melting of paraffin in the symmetrical plane, especially in the lower half of the symmetrical plane.

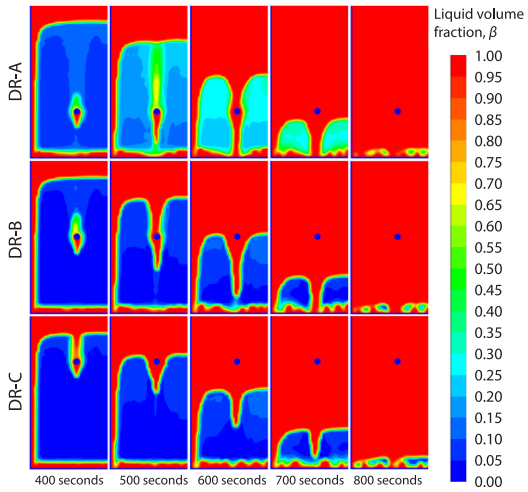

Figure 8. Variation of liquid volume fraction with double fins

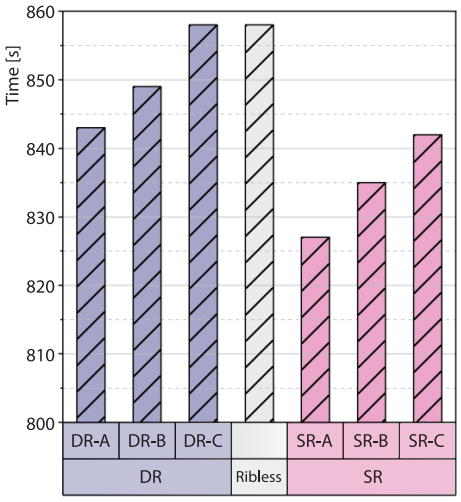

Figure 9. Paraffin melting time

Conclusions

This article establishes a simulation model for a plate type phase change energy storage unit, verifies the accuracy of the model, and uses it to simulate and study the paraffin phase change heat transfer process. The research results of this article can guide the design and performance optimization of P-PCESU, and improve its application value. The relevant conclusions are as follows.

- When there are no ribs, the melting time of paraffin in the P-PCESU is 858 seconds. The $\overline{Nu}$ in the energy storage unit decreases sharply with the increase of liquid volume fraction, and then slowly decreases. The melting time after adding a single rib is 827-842 seconds, and the melting time after adding a DR is 843-858 seconds. The rib has a promoting effect on the melting of paraffin in the PCESU.
- The melting time of the SR group is lower than that of the DR group, so adding ribs at the central section of the P-PCESU can effectively improve the melting speed of the phase change material.
- The SR-A located below the center section of the energy storage unit has the greatest effect on paraffin melting. To strengthen the phase change heat transfer process in the P-PCESU, the key is to strengthen the heat conduction and natural convection in the lower half of the symmetrical surface.

Acknowledgement

This Work is supported by the Special Fund of Hubei Longzhong Laboratory of Xiangyang Science and Technology Plan, the Hubei Natural Science Foundation Innovation and Development Joint Fund Project (2022CFD083), the Key Program of Xiangyang Technology project (High Tech Field) (2021ABH004233), and Distinctive Discipline Group of *New Energy Vehicle and Smart Transportation*.

Nomenclature

c_p – specific heat capacity of paraffin, [kJkg^{-1}K^{-1}]
H – specific enthalpy, [kJkg^{-1}]
H_{PCM} – height of the phase change unit, [m]
ΔH – latent enthalpy, [kJkg^{-1}]
h – the sensible enthalpy, [kJkg^{-1}]
h_{ref} – enthalpy at the reference temperature [kJkg^{-1}]
L – latent heat of phase transition of paraffin, [kJkg^{-1}]
Nu – Nusselt number
p – pressure, [Pa]
S_h – source term of the energy equation, [kJm^{-3}s^{-1}]
S_u – source term of the momentum equation in x-direction
S_v – source term of the momentum equation in y-direction
S_w – source term of the momentum equation in z-direction
T_ℓ – liquidus temperature of the material, [K]
T_{ref} – reference temperature, [K]
T_s – solidus temperature of the material, [K]
u – component of velocity in x-direction, [ms^{-1}]
v – component of velocity in y-direction, [ms^{-1}]
W_{PCM} – width of the phase change element, [m]
w – component of velocity in z-direction, [ms^{-1}]

Greek symbols

α – thermal expansion coefficient, [K^{-1}]
β – volume fraction of liquid paraffin
λ – thermal conductivity of paraffin wax, [Wm^{-1}K^{-1}]
μ – dynamic viscosity of paraffin wax, [Pa·s]
ρ – density of paraffin wax, [kgm^{-3}]

References

[1] Zong, H., *et al.*, Numerical Simulation on the Thermal Performance of the Cascade Stage Latent Thermal Storage System with the Various Phase Change Material (in Chinese), *Renewable Energy Resources*, *39* (2021), 05, pp. 618-625
[2] Mao, Q., Recent Developments in Geometrical Configurations of Thermal Energy Storage for Concentrating Solar Power Plant, *Renewable and Sustainable Energy Reviews*, *59* (2016), 105833
[3] Leite da Cunha, S. R., Barroso de Aguiar, J. L., Phase Change Materials and Energy Efficiency of Buildings: A Review of Knowledge, *Journal of Energy Storage*, *27* (2020), 101083
[4] Dong, Y., *et al.*, Review of Latent Thermal Energy Storage Systems for Solar Air-Conditioning Systems, *International Journal of Energy Research*, *44* (2020), pp. 669-707
[5] Kalidasan, B., *et al*., Phase Change Materials Integrated Solar Thermal Energy Systems: Global Trends and Current Practices in Experimental Approaches, *Journal of Energy Storage*, *27* (2020), 101118
[6] Guelpa, E., Verda, V., Thermal Energy Storage in District Heating and Cooling Systems: A Review, *Applied Energy*, *252* (2019), 113474
[7] Li, Z., *et al*., Applications and Technological Challenges for Heat Recovery, Storage and Utilisation with Latent Thermal Energy Storage, *Applied Energy*, *283* (2021), 116277
[8] Moreno, P., *et al*., The Use of Phase Change Materials in Domestic Heat Pump and Air-Conditioning Systems for Short Term Storage: A Review, *Renewable and Sustainable Energy Reviews*, *39* (2014), Nov., pp. 1-13
[9] Al-Aifan, B., *et al*., Performance Evaluation of a Combined Variable Refrigerant Volume and Cool Thermal Energy Storage System for Air Conditioning Applications, *International Journal of Refrigeration-Revue Internationale Du Froid*, *76* (2017), Apr., pp. 271-295
[10] Li, J., *et al.*, Thermal Performance of a Plate-Type Latent Heat Thermal Energy Storage Heat Exchanger – An Experimental Investigation and Simulation Study, *Journal of Energy Storage*, *65* (2023), 107295
[11] Zhu, X., *et al*., Heat Transfer Enhancement Technology for Ribs in Phase Change Energy Storage, *Journal of Energy Storage*, *55* (2022), 105833
[12] Zhou, H., *et al.*, Numerical Simulation of Internal Heat Transfer Characteristics in a Shell and Tube Cascade Phase Change Heat Storage Device Used in Mariculture (in Chinese), *Journal of Dalian Ocean University*, *35* (2020), 4, pp. 599-606
[13] Yang, J., *et al.*, Visualized Experiment on Dynamic Thermal Behavior of Phase Change Material in Metal Foam (in Chinese), *CIESC Journal*, *66* (2015), 2, pp. 497-503
[14] Wang, H., *et al*., Visualized Experiment on Solid-Liquid Phase Change Heat Transfer Enhancement with Multiple PCM (in Chinese), *CIESC Journal*, *70* (2019), 4, pp. 1263-1271+1662
[15] Shafee, A., *et al*., Phase Change Process of Nanoparticle Enhanced PCM in a Heat Storage Including Unsteady Conduction, *Journal of Molecular Liquids*, *309* (2020), 113102
[16] Kamkari, B., *et al.*, Experimental Investigation of the Effect of Inclination Angle on Convection-Driven Melting of Phase Change Material in a Rectangular Enclosure, *International Journal of Heat and Mass Transfer, 72* (2014), May, pp. 186-200

[17] Gurel, B., Thermal Performance Evaluation for Solidification Process of Latent Heat Thermal Energy Storage in a Corrugated Plate Heat Exchanger, *Applied Thermal Engineering*, *174* (2020), 115312
[18] Lin, W., *et al*., Experimental Study of the Thermal Performance of a Novel Plate Type Heat Exchanger with Phase Change Material, *Applied Thermal Engineering*, *178* (2020), 115630
[19] Voller, V. R., Prakash, C., A Fixed Grid Numerical Modelling Methodology for Convection-Difusion Mushy Region Phase-Change Problems, *Pergamon*, *30* (1987), 8, pp. 1709-1719
[20] Voller, V. R., Swaminathan, C. R., Eral Source-Based Method for Solidification Phase Change, Numerical Heat Transfer, Part B: *Fundamentals*, *19* (1991), 2, pp. 175-189
[21] Yuan, Y., *et al*., Melting Behaviors of Capric Acid in Rectangular Enclosure (in Chinese), *Journal of Southwest Jiaotong University*, *47* (2012), 2, pp. 236-240

Paper submitted: August 28, 2023
Paper revised: January 20, 2024
Paper accepted: January 23, 2024